Geometry flavored topological skeletons: Applications to shape handling, segmentation and retrieval

Julien Tierny, Jean-Philippe Vandeborre, Mohamed Daoudi
TELECOM Lille 1 / LIFL / USTL (France)
{*julien.tierny, jean-philippe.vandeborre, mohamed.daoudi*}@*lifl.fr*

Abstract

This paper reviews recent advances in 3D shape topological description aiming at enhancing standard topological approaches with shape geometry study. In particular, a new concise, invariant and high-level shape abstraction is proposed, namely the *enhanced topological skeletons*. This representation does not only encode the topological evolution of some Morse function level sets but also encode, in a unified manner, their geometrical evolution.

Applications to content handling, understanding and retrieval are presented and demonstrate the applicative interest of such a description for the management of large libraries of 3D shapes.

Categories and Subject Descriptors

H.3.1 [Information Storage and Retrieval]: Content Analysis and Indexing; I.3.5 [Computer Graphics]: Computational Geometry and Object Modeling;

Keywords

3D shape, shape analysis, shape retrieval, shape skeleton, shape segmentation, Reeb graph, Morse theory.

1 Introduction

Thanks to the recent advances in their visualization and acquisition, 3D shapes are becoming a media of major importance. These advances have led to an explosion in the number of available 3D shapes, both over the Internet or in specific-context databases such as computer-aided-design, medical or cultural heritage shape collections.

However, most of the time, 3D shapes are represented by raw boundary models (especially surface triangular mesh models) with no high-level geometrical information, such as shape internal structure, possible articulations, degrees of freedom, etc.

To handle the amount of data provided by 3D shape collections, high-level invariant shape descriptions first have to be extracted from their raw representation so as to enable efficient document processing tasks such as comparison, classification, edition, etc.

Research in the field of shape analysis has provided several tools for shape understanding and handling, such as spectral analysis [8, 12] or multi-resolution description [16]. Among the proposed approaches, topology based methods aim at investigating the topological properties of 3D shapes represented by manifold surfaces embedded in $\mathbb{R}^3$, in order to reveal the *structure* of the shape. In particular, Reeb graphs [15] are symbolic and skeletal representations of manifolds that give an interesting overview of the shape structure. Such descriptions have been used for several 3D shape processing tasks. Hilaga et al. [7] were the first authors to propose to use Reeb graphs as indexing key for fast comparison of items in large collections of 3D shapes. Zhang et al. [24] proposed to exploit the structural information provided by Reeb graphs to segment input shapes for content enhancing tasks such as texture mapping (where shape geometrical information is enriched with textural information). Aujay et al. [1] propose to enhance the standard Reeb graphs with anatomical information so as to shift shape topological skeletons into shape anatomical skeletons for realistic character animation.

In this paper, we present a new shape abstraction derived from topological skeletons (Reeb graphs), called *enhanced topological skeletons* which aims not only at describing the surface topology (or shape structure) but also its geometry in a unified manner. First, we recall Reeb graph's theoretical background and then we introduce the notion of enhanced topological skeleton. Secondly, we demonstrate the applicative interest of such a shape representation for the management of large libraries of 3D shapes by describing a wide panorama of experimented applications, such as shape deformation, semantic segmentation or retrieval.

2 Enhanced topological skeletons

Before introducing the contribution of this work, namely the *enhanced topological skeletons*, we first define the mathematical entities corresponding to the initial representations of 3D shapes in shape collections. Then, we progressively introduce important results from differential topology for the extraction of shape topological invariants. Then we introduce Reeb graphs and shift from topological invariant shape description to high-level invariant shape description. Finally, *enhanced topological skeletons* are presented, enriching the high-level description proposed so far by standard Reeb graphs.

2.1 Differentiable manifolds

The most common representation representation of a 3D shape is the triangle surface mesh model. In this framework, only the surface of the shape is represented by a triangular mesh. From a mathematical point of view, such representations correspond to simplicial decompositions of 2-manifolds embedded in $\mathbb{R}^3$.

Definition 1 (Manifold) *A topological space $\mathbb{X}$ is a k-*manifold *if for each point $p \in \mathbb{X}$ there exists a neighborhood $N \in \mathbb{X}$ which is homeomorphic to $\mathbb{R}^k$.*

Roughly speaking, a manifold space is a curve space which can be locally approximated by an Euclidean space. In the case of 3D shapes, manifolds of dimension 2 are considered, and especially 2-manifolds that can be embedded in *human space* ($\mathbb{R}^3$). In practice, 2-manifold surfaces are point-sampled and points are linked together to form triangles. Then the manifold surface is approximated by its simplicial decomposition, named triangulation. In the following paragraphs, the rest of the discussion will be held in the continuous case (considered entities will be manifolds) but results reported here have been extended to the discrete case [2] (where considered entities are triangulations).

2.2 Morse theory

Morse theory investigates the relations between the topological invariants of a manifold and the properties of a particular class of smooth functions defined over such a manifold, called the *Morse functions*. In the context of shape description, Morse theory provides a powerful and efficient framework for topology characterization.

2.2.1 Morse functions

The notion of Morse functions is closely related to the notion of critical points, that can be defined as follows:

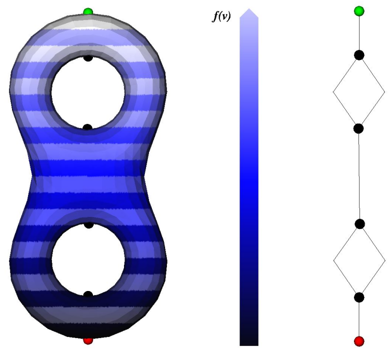

Figure 1: A Morse function defined on genus-2 2-manifold, its critical points and its Reeb graph.

Definition 2 (Critical point) *Let f be a smooth function defined on a compact manifold $\mathbb{M}$. A point $p \in \mathbb{M}$ is a critical point if f gradient vanishes in p.*

Definition 3 (Non-degenerate critical point) *A critical point p of a smooth function f defined on a manifold $\mathbb{M}$ is* non-degenerate *if the Hessian matrix of f is non singular in p.*

Definition 4 (Morse function) *Let f be a smooth function defined on a compact manifold $\mathbb{M}$. f is a* Morse function *if all its critical points are non-degenerate.*

As a consequence of the definition of Morse functions, in the case of 2-manifolds embedded in $\mathbb{R}^3$, a Morse functions can only admit three types of critical points: local minima, local maxima and saddles. Figure 1 gives an example of a Morse function f (defined by the height function) on a bi-torus. f critical points have been displayed respectively in green, red and black for local maxima, local minima and saddles.

2.2.2 Morse theory results

Two important results from Morse theory [13] (which have been extended to the discrete case by Banchoff [2]) are worth being mentioned here.

First, Morse functions are everywhere dense in the space of smooth functions (defined on a given manifold $\mathbb{M}$). As a consequence, any smooth function on a manifold can be transformed into a Morse function by a slight perturbation, which transforms degenerate critical points into non-degenerate ones. This first result has a very important practical impact: in practice, any smooth function computed on triangular mesh can easily benefit from Morse function properties.

Secondly, the most important result of Morse theory for topology characterization is the Morse-Euler formula, where k is the dimension of the manifold ($k = 2$ for 3D shapes):

$$\chi_{\mathbb{M}} = \sum_{i=0}^{k} (-1)^i \mu_i(f) = \mu_0(f) - \mu_1(f) + \mu_2(f) \tag{1}$$

In equation 1, $\mu_i(f)$ stands for the i^{th} Morse number of f, which is equal to the number of f critical points of index i. In particular, $\mu_0(f)$, $\mu_1(f)$ and $\mu_2(f)$ are respectively the number of f local minima, saddles and maxima. This equation states that the Euler-Poincaré characteristic $\chi_{\mathbb{M}}$ of a manifold $\mathbb{M}$ (which is a topological invariant of $\mathbb{M}$ related to its genus) can be derived by the types and numbers of f critical points. In practice, simple algorithms [4] enable the identification of f critical points, and thus the extraction of the topological invariants of the shapes, in linear time (with the number of vertices in the mesh).

2.3 Reeb graph

Morse theory provides simple and efficient tools for the extraction of the topological invariants of the shapes. Reeb graphs [15] are a symbolic representation of the shape which is based on Morse theory results and which extends its descriptive potential.

2.3.1 Reeb graph definition

Definition 5 (Reeb graph) *Let $f : \mathbb{M} \rightarrow \mathbb{R}$ be a Morse function defined on a compact manifold $\mathbb{M}$. The Reeb graph $R(f)$ is the quotient space on $\mathbb{M} \times \mathbb{R}$ by the equivalence relation $(p_1, f(p_1)) \sim (p_2, f(p_2))$, which holds if $f(p_1) = f(p_2)$ and p_1, p_2 belong to the same connected component of $f^{-1}(f(p_1))$.*

The Reeb graph is a simplicial complex that contracts and represents the connected components of the level sets of f by single vertices (single equivalence classes). Roughly speaking, the Reeb graph depicts the evolution of the topology of f level sets as f evolves. As shown in figure 1, the Reeb graph keeps track of the connectivity relations of f critical points, revealing the structure of the manifold between these points.

2.3.2 Results

Cole-McLaughlin et al. [4] extended the Morse-Euler formula to general 2-manifolds (orientable or not, with or without boundary components) and proved additional relations between the number of loops $L(R(f))$ of the Reeb graph $R(f)$ and the topology of the manifold. In the case of orientable 2-manifolds (which corresponds to the case of 3D shapes), the genus g is equal to the number of loops $L(R(f))$ if $\mathbb{M}$ has no boundary components. If $\mathbb{M}$ has $b_{\mathbb{M}}$ boundary components, then $g \leq L(R(f)) \leq 2 \times g + b_{\mathbb{M}} - 1$. These results show that Reeb graphs provide an even better understanding of the manifold structure than former Morse theory.

Moreover, Reeb graphs give a symbolic and skeletal representation of the manifold structure, which constitutes a higher-level description of the manifold than the original surface representation. However, even if it gives a full topological understanding of the shape, it does not encode its geometry.

2.4 Enhanced topological skeletons

Enhanced topological skeletons were first introduced in [18] (and then further developed in [22, 21, 20]) to overcome the above issue and to describe both the manifold topological and geometrical structure in a unified manner. In particular, enhanced topological skeletons not only describe the topological evolution of f level sets but also their geometrical evolution, through an additional measuring function, denoted as g.

2.4.1 Definition

Definition 6 (Geometrical measuring function) *Let $R(f)$ be the Reeb graph of a Morse function f defined on a compact close 2-manifold $\mathbb{M}$. Let g be a smooth function that maps each equivalence class c of $R(f)$ to $\mathbb{R}$ ($g : R(f) \rightarrow \mathbb{R}$). g is referred to the geometrical measuring function of $R(f)$. f is referred to the topological measuring function of $R(f)$.*

Definition 7 (Enhanced topological skeleton) *Let f be a Morse function defined on a compact manifold $\mathbb{M}$ and $R(f)$ its Reeb graph. Let g be a measuring function of $R(f)$. The enhanced topological skeleton noted $E(f, g)$ is the couple $(R(f), g(R(f)))$.*

The enhanced topological skeleton $E(f, g)$ is, like the Reeb graph, a simplicial complex which contracts connected components of f level sets to equivalence classes. Moreover, every equivalence class (every contour) $c \in R(f)$ is associated with a real value $g(c)$ which concisely encodes the geometrical evolution of f level sets.

2.4.2 Algorithms

The Reeb graph sub-jacent to the enhanced topological skeleton can be computed with any Reeb graph construction algorithm [4, 19, 14]. Basically, that kind of algorithms sweep the manifold represented by a triangulation T from f minima to its maxima and keeps track of the de-connection and re-connection of f level sets. At each step of the sweeping process, the measuring function g has to be evaluated on each contour (each equivalent class $c \in R(f)$). As the number of vertices on a contour is a function of the overall number of vertices in T, this measurement requires $O(n)$ steps, with n the number of vertices in T. Standard Reeb graph construction algorithms require $O(n \times log(n))$ steps. Consequently to g evaluation, the enhanced topological skeleton construction requires $O(n^2 \times log(n))$ steps.

2.4.3 Results

Depending on what is expected to be revealed in the shape, several functions can be chosen for f and g. For example, for terrain modeling, the height function (f) will present critical points over hills and valleys, providing an appropriate topological description. In order to guarantee the invariance of the skeleton with regard to a certain class of transformations, employed metrics for function measures should be invariant to these specific transformations. As an example, geodesic distances (distances between two points along the surface) are invariant to rigid transformations and robust to non-rigid ones. Consequently, in order to compute enhanced topological skeletons invariant to rigid transformations and robust to non-rigid ones, f and g must be based on geodesic distances. As an example, in [11], the f function is defined with regard to the geodesic distance from a source vertex.

As for the geometrical measuring function g, for example, the geodesic perimeter of f contours can be computed to keep track of the thinness evolution of the manifold with regard to f evolution. In such a case, g critical points correspond to curvature transitions on the surface, and in particular, its local minima correspond to the surface constrictions [6]. Based on this result, enhanced topological skeletons were first propose in the framework of character animation to enhance the high level description provided by Reeb graphs to furthermore detect geometrical criticalities corresponding to potential articulations, as described in the next section.

3 Shape deformation

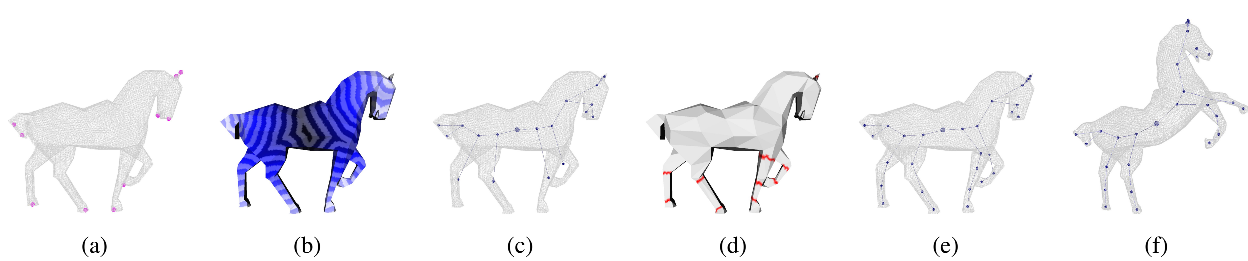

Figure 2: Deformation skeleton based on enhanced topological skeleton extraction [18]. (a) Feature points (b) f function (c) Reeb graph (d) constrictions (e,f) deformation skeletons.

Thanks to the high level and more descriptive representation provided by enhanced topological skeletons, content handling (in particular mesh deformation) has been proposed in a previous work [18].

When dealing with character animation, potential articulations are located at the basis of the components (like the shoulders of a humanoid) or at the bottlenecks of the surface (like the elbows, the wrists or the phalanxes). Consequently, a deformation skeleton has been proposed by subdividing the conventional Reeb graph along surface constrictions (fig. 2(d)).

In particular, the topological measuring function employed (the f function, fig. 2(b)) has been defined for each vertex of the mesh as the geodesic distance to the closest feature point (fig. 2(a)). Feature points can be extracted automatically [9, 18, 12]. Here, the algorithm proposed in [18] has been employed. Such a f function guarantees the enhanced topological skeleton to be invariant to rigid transformations and to be robust against non-rigid ones. Moreover, as feature points give a good preview of the shape structure, only the meaningful parts of the object are identified in the Reeb graph (fig. 2(c)).

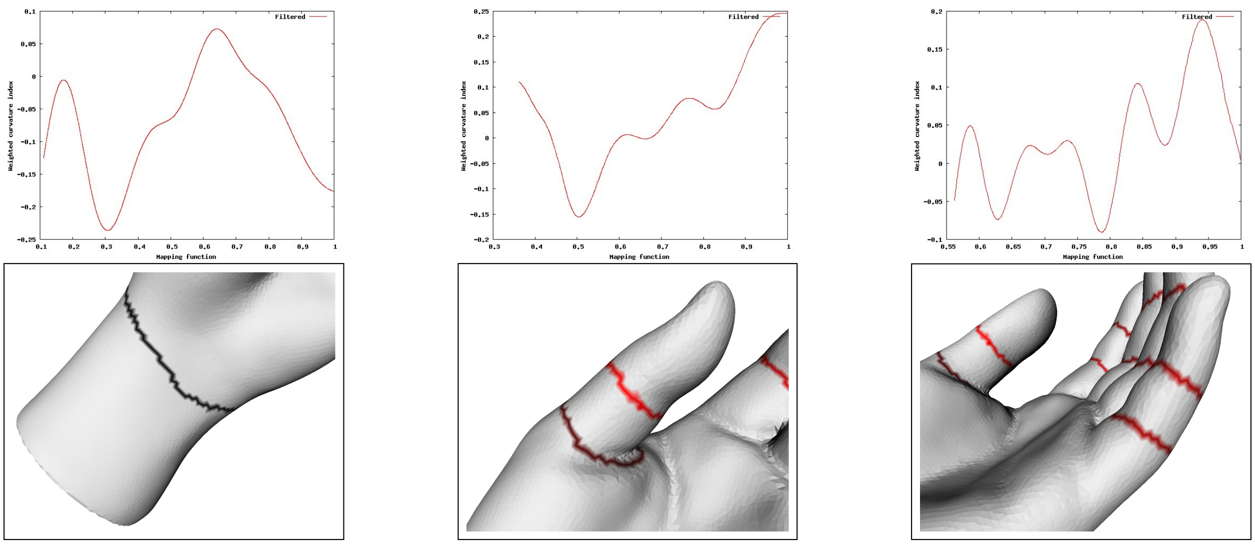

Figure 3: Geometrical measuring function g along Reeb graph edges (first line) and its corresponding surface connected components (second line).

As for the geometrical measuring function g, $g(c)$ is estimated by computing the Discrete Gaussian Curvature in each of the vertices of the contour c (connected component of f level lines). The overall approach has been further developed in [22], where, in particular, an improved computation of contour curvature has been proposed:

$$g(c) = \frac{\sum_{\forall v \in c} I_c(v) \times (\mathcal{L}_{e_1}(v) + \mathcal{L}_{e_2}(v))}{2 \times \mathcal{P}(c)} \tag{2}$$

Where $\mathcal{P}(c)$ stands for the perimeter of the contour c, $\mathcal{L}_{e_1}(v)$ and $\mathcal{L}_{e_2}(v)$ for the lengths of the edges adjacent to v on the contour and $I_c(v)$ for the curvature index [10] in v. Such a computation is much more stable against variation in the surface mesh sampling [22]. Figure 3 shows the evolution of the g function over particular edges of the Reeb graphs and the corresponding surface connected components. In the curve of the first line, the topological measuring function f is reported on the X-axis while the geometrical measuring function g is reported on the Y-axis. Roughly speaking, these curves depict the curvature evolution of f level sets from the components basis to their extremity. Local minima of g correspond to surface constrictions while local maxima of g correspond to configurations where the object gets larger.

In order to detect the potential articulations (for character deformation), surface constrictions (which are highly concave configurations) have to be identified. Consequently, g negative local minima are identified as

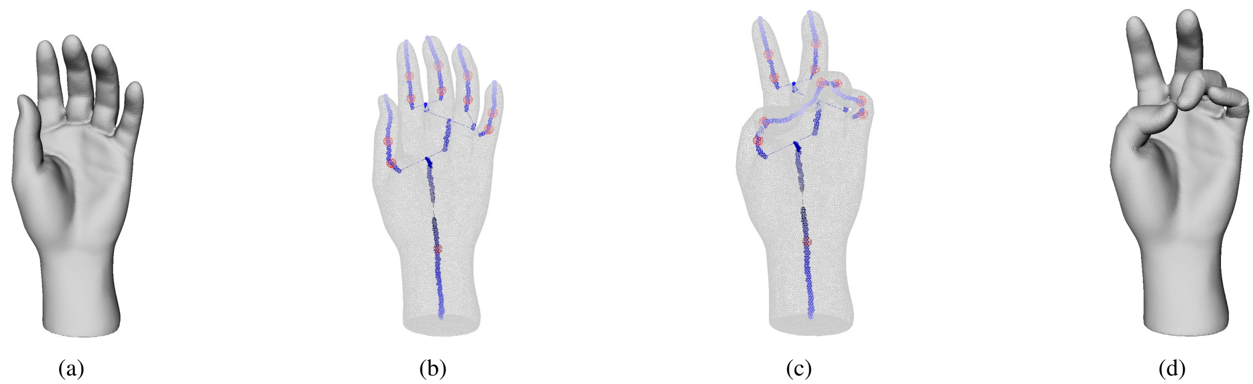

Figure 4: Application of enhanced topological skeleton to content handling (surface deformation): the user grabs the branches of the skeleton to the desired position and the deformation is automatically transferred to the surface.

constrictions, as reported by red curves in figure 3 (second line). Next, a deformation skeleton is proposed by sub-dividing the edges of the Reeb graphs along surface constrictions (fig. 2(e)).

Finally, within the framework of content handling (and particularly deformation), the user just grabs the branches of the enhanced topological skeleton to the desired deformed position, using constrictions special nodes (in red in figure 4) as articulations. Then, thanks to the equivalence relation between the nodes of the enhanced topological skeleton and the mesh, the deformation is automatically transferred to the mesh, as illustrated in figure 4.

4 Semantic oriented segmentation

Shape segmentation is a major task in shape understanding. It consists in subdividing a surface into patches of uniform properties, either from a strictly geometrical point of view or from a more *perceptual* point of view. This operation has become a necessary pre-processing tool for various human shape interaction tasks such as texture mapping or modeling. Recently, the need for *compatible segmentation* - which means segmenting identically two surfaces representing the same class of object - has been expressed [9]. Contrary to low-level based approaches, a solution to this problem resides in driving the segmentation process using high-level notions such as defined in human perception theory [3].

Figure 5: Semantic oriented segmentation process [21].

In a previous work [21], the problem of compatible semantic oriented segmentation has been addressed using enhanced topological skeletons. The first stage of this work was to extract a pre-segmentation skeleton, using the same approach as in the framework of shape deformation [22] (same f and g functions and sub-division along constrictions), as illustrated in figure 5(a). By subdividing the surface mesh along constrictions and Reeb graph edges boundaries, a raw segmentation is obtained (fig. 5(b)). Then, heuristics based on perceptual considerations drives a skeleton simplification process, by merging thin identified surface patches with bigger neighboring ones (fig. 5(c)). This simplification process results in a fine semantic oriented segmentation of the object, segmenting for example the hand into palm, fingers and phalanxes (fig. 5(d)).

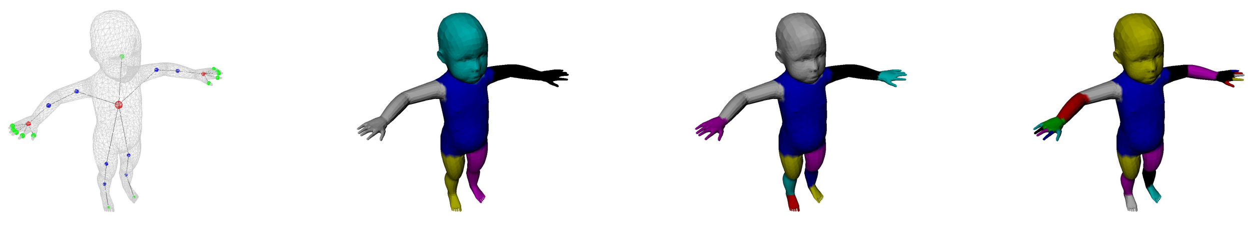

(a) (b) (c) (d)

Figure 6: Hierarchy of segmentations based on topological criteria [21].

Moreover, a progressive understanding of the shape is provided by a hierarchy of segmentations based on topological criteria. The basic idea behind this hiearchical scheme is to sweep the simplified skeleton (fig. 6(a)) from its central node (big sphere in red) and to recursively subdivide branches of the skeleton in priority along nodes of high cardinality (corresponding to topological variations). Thanks to the strategy, in figure 6, at the first level of the hierarchy, the humanoid is segmented into core and limbs. Next, at the second level, limbs are subdivided in priority along topological transitions (divided into arms and hands for example). Then, the final level of the hierarchy is achieved when the surface patches cannot be further subdivided according to the simplified skeleton (fig. 6(a)).

5 Shape retrieval by parts

In term of management of 3D shape collections, shape retrieval is a major challenge. In such an application, the system is queried with a 3D example object and is expected to retrieve in the collection the most visually similar shapes. Surface parameterization based shape comparison approaches have shown to provide very accurate results [23] in the framework of face recognition. However, their major drawback is that the surfaces to compare must be topology equivalent.

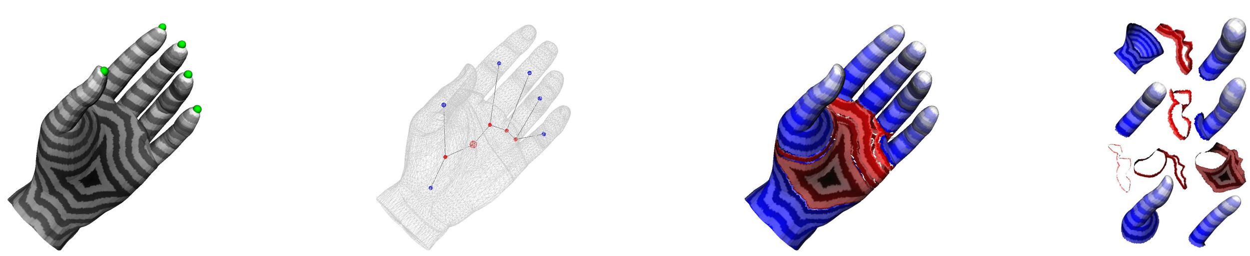

(a) (b) (c) (d)

Figure 7: Reeb chart segmentation process [20].

Using a divide and conquer strategy based on Reeb graphs, a novel approach for shape retrieval by parts has been proposed [20]. This work proposes to segment the shape into distinctive *Reeb charts* using its Reeb graph. Then, the similarity between two shapes is evaluated by computing the similarity between the Reeb charts, thanks to their geometrical measuring function g. In particular, it has been proved [20] that Reeb graph segmentation provides only two kinds of charts: disk-like or annulus-like Reeb charts (respectively in blue and red in figure 7). As the topology of the sub-parts to compare is fully controlled, then parameterization techniques can be employed for the g function computation.

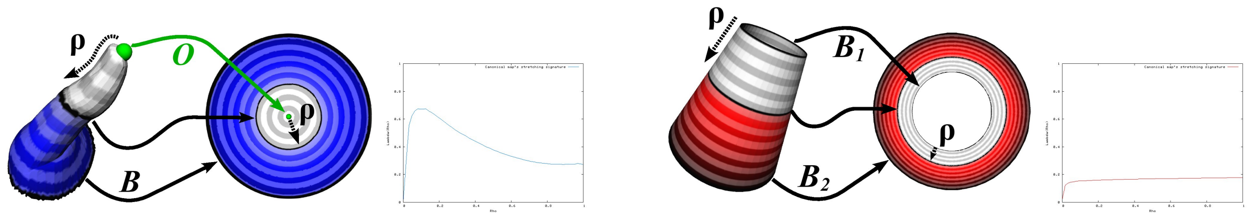

(a) (b) (c) (d)

Figure 8: Disk-like and annulus-like chart unfolding and signature computation processes [20].

In particular, we propose to map each chart to the canonical planar domain (either the unit disk or the unit annulus). Then the evolution along f of the area distortion of such a mapping is computed as the geometrical measuring function g (fig. 8). Finally, the geometrical distance between two charts is given by a L_1 distance.

(a) Query. (b) d = 0.89 (c) d = 1.13 (d) d = 1.30 (e) d = 1.47 (f) d = 1.61 (g) d = 1.77 (h) d = 1.85

Figure 9: Chart similarity matchings between a horse query model and retrieved results.

Such a shape similarity estimation strategy has been experimented on the ISDB data-set, which is composed of 106 articulated models. Figure 9 shows a typical query and the results retrieved by the system. The charts that have been matched together (with regard to their g function) have been displayed with the same color. Notice that, for example, the tail of the horse query model has been matched with the tail of each retrieved results, which demonstrates the efficiency of the proposed part signature. Moreover, this figure shows that the proposed signature is clearly pose-insensitive since horses in different poses have been retrieved as the top results.

Methods	NN	1^{st} T.	2^{nd} T.	E-M	DCG
RCU	**94.3 %**	**79.2 %**	**89.4 %**	**59.1 %**	**92.1 %**
HBA	88.7 %	70.6%	85.7 %	54.0 %	89.1 %
[5]	67.9 %	44.0 %	60.6 %	39.4 %	71.7 %

Table 1: Similarity estimation scores on the ISDB dataset.

Table 1 gives a more quantitative evaluation of the system, with comparison to other techniques (the higher the scores are the better they are, see [17]). The first line reports the scores of our comparison algorithm, using Reeb chart unfolding signatures. The second one reports the scores of the same algorithm, using the sub-part attributes proposed in [7] (area ratio and Morse interval length). For example, with 1^{st} Tier score, the gain provided by Reeb chart unfolding signatures is about **9 %**.

6 Conclusion

In this paper, we presented a new concise, invariant and high-level shape abstraction called *enhanced topological skeletons*. This representation improves previous topological descriptions by encoding in a unified manner the shape topology and geometry. It both describes some Morse function level sets topological and geometrical evolution.

Applications to content handling, segmentation and retrieval were presented and demonstrated the applicative interest of such a representation for the management of large libraries of 3D shapes.

In the future, we would like to extend the theoretical framework of enhanced topological skeletons to higher dimension manifolds, so as to efficiently encode and describe dynamic shapes (3D plus time) and thus enable their management in digital collections.

References

[1] Grégoire Aujay, Franck Hétroy, Francis Lazarus, and Christine Depraz. Harmonic skeleton for realistic character animation. In *ACM/EG Symposium on Computer Animation*, pages 151–160, 2007.

[2] T.F. Banchoff. Critical points and curvature for embedded polyhedra. *Journal of Differential Geometry*, 1:245–256, 1967.

[3] Irving Biederman. Recognition-by-components: A theory of human image understanding. *Psychological Review*, 94:115–147, 1987.

[4] Kree Cole-McLaughlin, Herbert Edelsbrunner, John Harer, Vijay Natarajan, and Valerio Pascucci. Loops in Reeb graphs of 2-manifolds. In *Symposium on Computational Geometry*, pages 344–350, 2003.

[5] Thomas Funkhouser, Patrick Min, Michael Kazhdan, Joyce Chen, Alex Halderman, and David Dobkin. A search engine for 3D models. *ACM Transactions on Graphics*, 22:83–105, 2003.

[6] Franck Hétroy. Constriction computation using surface curvature. In *Eurographics*, pages 1–4, 2005.

[7] Masaki Hilaga, Yoshihisa Shinagawa, Taku Kohmura, and Tosiyasu Kunii. Topology matching for fully automatic similarity estimation of 3D shapes. In *SIGGRAPH*, pages 203–212, 2001.

[8] Varun Jain and Hao Zhang. A spectral approach to shape-based retrieval of articulated 3D models. *Computer-Aided Design Journal*, 39:398–407, 2007.

[9] Sagi Katz, George Leifman, and Ayellet Tal. Mesh segmentation using feature point and core extraction. *The Visual Computer*, 21:865–875, 2005.

[10] Jan J Koenderink and Andrea J van Doorn. Surface shape and curvature scales. *Image and Vision Computing*, 10:557–565, 1992.

[11] Francis Lazarus and Anne Verroust. Level set diagrams of polyhedral objects. Technical Report 3546, Institut National de Recherche en Informatique et en Automatique (INRIA), 1999.

[12] R. Liu and H. Zhang. Mesh segmentation via spectral embedding and contour analysis. *Computer Graphics Forum*, 26:385–394, 2007.

[13] John Milnor. *Morse Theory*. Princeton University Press, 1963.

[14] V Pascucci, G Scorzelli, P T Bremer, and A Mascarenhas. Robust on-line computation of reeb graphs: simplicity and speed. *ACM Transactions on Graphics*, 26:58.1–58.9, 2007.

[15] Georges Reeb. Sur les points singuliers d'une forme de Pfaff complètement intégrable ou d'une fonction numérique. *Comptes-rendus des Séances de l'Académie des Sciences*, 222:847–849, 1946.

[16] Basile Sauvage, Stéfanie Hahmann, and Georges-Pierre Bonneau. Volume preservation of multiresolution meshes. *Computer Graphics Forum*, 26:275–283, 2007.

[17] Philip Shilane, Patrick Min, Michael Kazhdan, and Thomas Funkhouser. The Princeton shape benchmark. In *IEEE Shape Modeling International*, pages 167–178, 2004.

[18] Julien Tierny, Jean-Philippe Vandeborre, and Mohamed Daoudi. 3D mesh skeleton extraction using topological and geometrical analyses. In *Pacific Graphics*, pages 85–94, 2006.

[19] Julien Tierny, Jean-Philippe Vandeborre, and Mohamed Daoudi. Invariant high-level Reeb graphs of 3D polygonal meshes. In *IEEE 3DPVT*, pages 105–112, 2006.

[20] Julien Tierny, Jean-Philippe Vandeborre, and Mohamed Daoudi. Reeb chart unfolding based 3D shape signatures. In *Eurographics*, pages 13–16, 2007.

[21] Julien Tierny, Jean-Philippe Vandeborre, and Mohamed Daoudi. Topology driven 3D mesh hierarchical segmentation. In *IEEE Shape Modeling International*, pages 215–220, 2007.

[22] Julien Tierny, Jean-Philippe Vandeborre, and Mohamed Daoudi. Enhancing 3D mesh topological skeletons with discrete contour constrictions. *The Visual Computer*, To appear.

[23] Sen Wang, Yang Wang, Miao Jin, Xianfeng Gu, and Dimitris Samaras. 3D surface matching and recognition using conformal geometry. In *IEEE Computer Vision and Pattern Recognition*, pages 2453–2460, 2006.

[24] Eugene Zhang, Konstantin Mischaikow, and Greg Turk. Feature-based surface parametrization and texture mapping. *ACM Transactions on Graphics*, 24:1–27, 2005.